Nanotechnology Perceptions
ISSN 1660-6795
www.nano-ntp.com

Smart Impedance and Grid Forming Converter Supported d-STATCOM

Sushil Kumar Bhoi, Asini Kumar Baliarsingh, Jayanta Kumar Panigrahi

Department of Electrical Engineering, Government College of Engineering Kalahandi
Email: sushilkumarbhoi@gmail.com

The current paper explains the design and modeling of both smart impedance and grid-forming converters for the distributed static compensator (d-STATCOM). High impedance due to a greater number of distributed generations results in severe power quality (PQ) troubles like harmonic distortion and resonance problems. Hence, the selection and design of an LCL filter is required to suppress the PQ difficulties. However, it does not provide a significant contribution to the resonance. Hence, HAPF (Hybrid active power filter) is a rational choice to provide all types of compensation and allows better filtering performance. Both the use Smart Impedance and grid forming converter are used to modify the microgrid bus impedance to a quasi-infinite bus, while active power maintains the same. The purpose of this type of implementation is to enhance the power quality of micro grid. Several issues like harmonic reduction, voltage imbalance, and resonance problems are eradicated using this scheme. Experimental outcomes are offered to determine the efficiency of the suggested method.

Keywords: DSTATCOM, hybrid power filter, smart impedance, grid forming converter, power quality.

1. Introduction

In the early days, passive power filters were utilized to absorb/inject the reactive power for the different loading states. Since 1976, the active power filter (APF) has attained remarkable progress in dynamic compensation [1-9]. However, APF increases initial and ongoing costs because it needs $\sqrt{2}$ times the PCC voltage for the DC-link voltage to do the correction. Later, in 2003, Akagi et al. [10] suggested an LC-coupling HAPF with low dc-link operational voltage in an effort to lower the cost of APFs. Unfortunately, because of its limited compensation range, HAPF may lose its low inverter rating characteristic while running outside of its compensation range, necessitating a high DC-link operation voltage [11–15].

Distributed generator (DG) based microgrid systems have advanced quickly. Nevertheless, the erratic weather will have a significant influence on the DGs' output characteristics, which will damage the microgrid's PQ. By linking two microgrids with an active power conditioner (APC), it is possible to enhance the PQ on both ends. When a problem arises on one microgrid,

the APC on the other MG (Microgrid) can compensate for both active and reactive power. As a result, the APC is now required for microgrid applications. In contrast, back-to-back power converter topologies are among the most widely used in a variety of applications, including microgrids, traction power systems, wind power systems, and motor drivers. Thus, in this research, active and reactive power compensation is accomplished by a 3-phase back-to-back APC.

The microgrid is not as robust as the linked grid while it is functioning in islanded mode. Its voltage waveform may degrade in this case due to the drop in the harmonic voltage caused by the nonlinear load currents. These currents may also induce parallel resonances, which can result in harmonic over-voltages. Furthermore, a small distortion of the network voltage waveform to which Distributed Generation (DG) inverters are linked has a major impact on the quality of the current injected by these devices. Therefore, power conditioning action is necessary to provide acceptable PQ, which is necessary to ensure the transfer of the best energy from the DGs to the MG.

The research has suggested a number of methods for directly integrating PQ correction into DG inverter management algorithms. However, the installation of specialized power conditioning equipment, like active filters or STATCOMs, is required when the MG is running with converters that do not take PQ mitigation into consideration, and modification in their control might not be feasible. In this case, the hybrid filter architecture known as Smart Impedance could be used as a cost-efficient solution because it combines the flexibility of APF with a lower cost n comparison to regular active filters & STATCOMs.

The usage of smart impedance for microgrid PQ enhancement, voltage distortion reduction, load current harmonic compensation, and parallel resonance damping is covered in this paper. By doing these, the microgrids become less vulnerable to changes in load. This microgrid behaves more like a stiffer grid as a result of the Smart Impedance's action, which is comparable to a reduction in the source equivalent impedance at the PCC (Point of Common Coupling). In typical power grids, this impact is typically achieved by expanding the grid's generation capacity. Without adding additional generators to the microgrid, the application that is being discussed here exhibits comparable behavior. This compensated MG could be thought of as a kind of quasi-infinite bus. For nonlinear loads, it functions as an infinite bus.

The Smart Impedance's working concept and efficacy for displacement power factor (DPF) compensation and harmonic current mitigation have been demonstrated in earlier research. This research focuses on the implications of equivalent impedance reduction on voltage quality improvement in microgrids. The primary contribution of this work is the study of the system equivalent circuit, which demonstrates that the modification of the grid's equivalent impedance is efficient as well as marks a new development in smart impedance.

The microgrid is made up of the Smart Impedance, local loads, and a single-phase grid-forming converter that can function with both islanded and grid-connected loads. The expected quasi-infinite bus behavior is demonstrated by the experimental results obtained in this microgrid. Furthermore, a theoretical examination of the behavior of Smart Impedance is provided.

In recent years, HAPF has attained much attraction due to its significant contribution to the

distributed generation. This type of filter is more complex compared to a simple active power filter. Keeping in the mind resonance problem, the necessity of frequencies HAPF arises [16]. Several types of converters like LC or LCL are required to reduce the switching ripple. But LCL is chosen to provide better resonance frequencies compared to LC because of (the advantages of the LCL filter)[17-18].

The paper's structure is organized as follows: The circuit diagram of the system using both smart impedance and grid forming converter is described in Section II. Section III describes the design and modeling of the smart impedance converter. The design and modeling of the grid-forming converter is discussed in Section IV. Section V includes simulation results whereas Section VI includes experimental results. Finally, the conclusion of the paper is summarized in Section VI.

2. ISLANDED MICROGRID

Microgrids can function both in stand-alone and grid-connected modes, and they can switch between them. They can be set up and managed in a variety of ways, including hierarchically, decentralized, and centralized. This study employs a single master voltage-regulated converter in its microgrid topology. When in islanded mode, this converter—known as a grid-forming converter—maintains the microgrid's voltage, amplitude, and frequency. In the situation of voltage sags, grid failures, and extreme voltage/frequency fluctuations, this converter is also in charge of monitoring the grid's voltage & frequency and issuing commands to disconnect the microgrid. Other DG converters in this configuration are linked to the MG as grid-feeding converters, that are managed as current sources as well as give the loads active power. The majority of wind & solar power converters function in this way, meaning that they were programmed to output the most active electricity that is accessible. Grid-feeding converters are made to connect to the grid in parallel with other converters. But without a grid-forming converter, or the synchronous generator, that controls voltage amplitude along with the frequency, they cannot function on islanded microgrids. Because of this, the grid-forming converter voltage's quality has a critical impact on the functionality of this structure.

3. GRID-FORMING CONVERTER

It regulates the microgrid voltage's frequency and amplitude when it is in isolated mode. The amplitude, as well as frequency references, are maintained constant at every converter operating point due to the converter's isochronous control. This control is not the same as the droop control, which modifies the converter output voltage as well as frequency in response to variations in the reactive & active power of the load. An internal oscillator maintains a fixed voltage frequency of 60 Hz in the islanded mode. The voltage amplitude control technique has been depicted in Fig. 2. The fundamental voltage amplitude (AVC), attained utilizing “a Modified Synchronous Reference Frame, in comparison with the reference value (AVref). A PI (Proportional Integral) controller creates the control signal (u), which is multiplied by the unity vector sin(ωt), creating the voltage reference signal (Vref). The IGBT’s (‘Insulated-Gate Bipolar Transistor’) dead-time impact is compensated utilizing the average value technique.

4. SMART IMPEDANCE

An effective substitute for enhancing PQ in MGs is the hybrid filter. A tuned passive cell is not required with the Smart Impedance Hybrid Filter design, which comprises an active filter in series with a capacitor bank. The" equivalent impedance of the Smart Impedance must be extremely low in order to stop harmonic current from entering the grid-forming converter and instead directing it into the filter-branch rather than the voltage source. Since the passive portion of the Smart Impedance is made up of a bank of capacitors, an inductive reactance needs to be built in order to electrically tune the Smart Impedance for a certain frequency. With distinct active reactances for every desired harmonic, the topology may accomplish several tuning frequencies simultaneously. Additionally, it generates an active resistance to remove the branch's residual resistance and turn it into the perfect tuned filter. However, the hybrid branch can reduce series resonances between the passive filter circuit and source impedance by offering infinite impedance for source voltage harmonics.

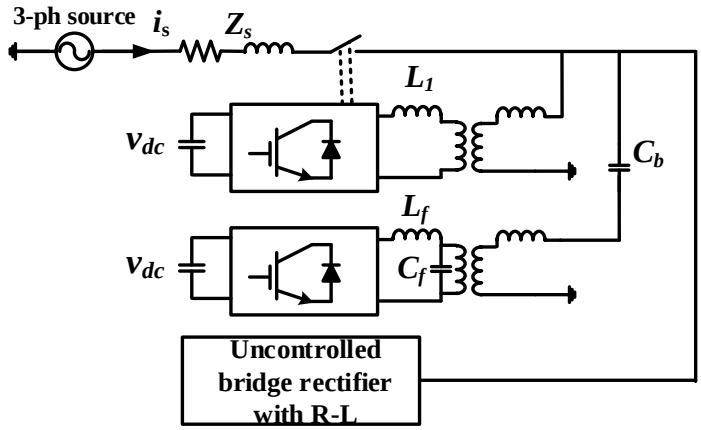

Fig. 1. Bridge Rectifier

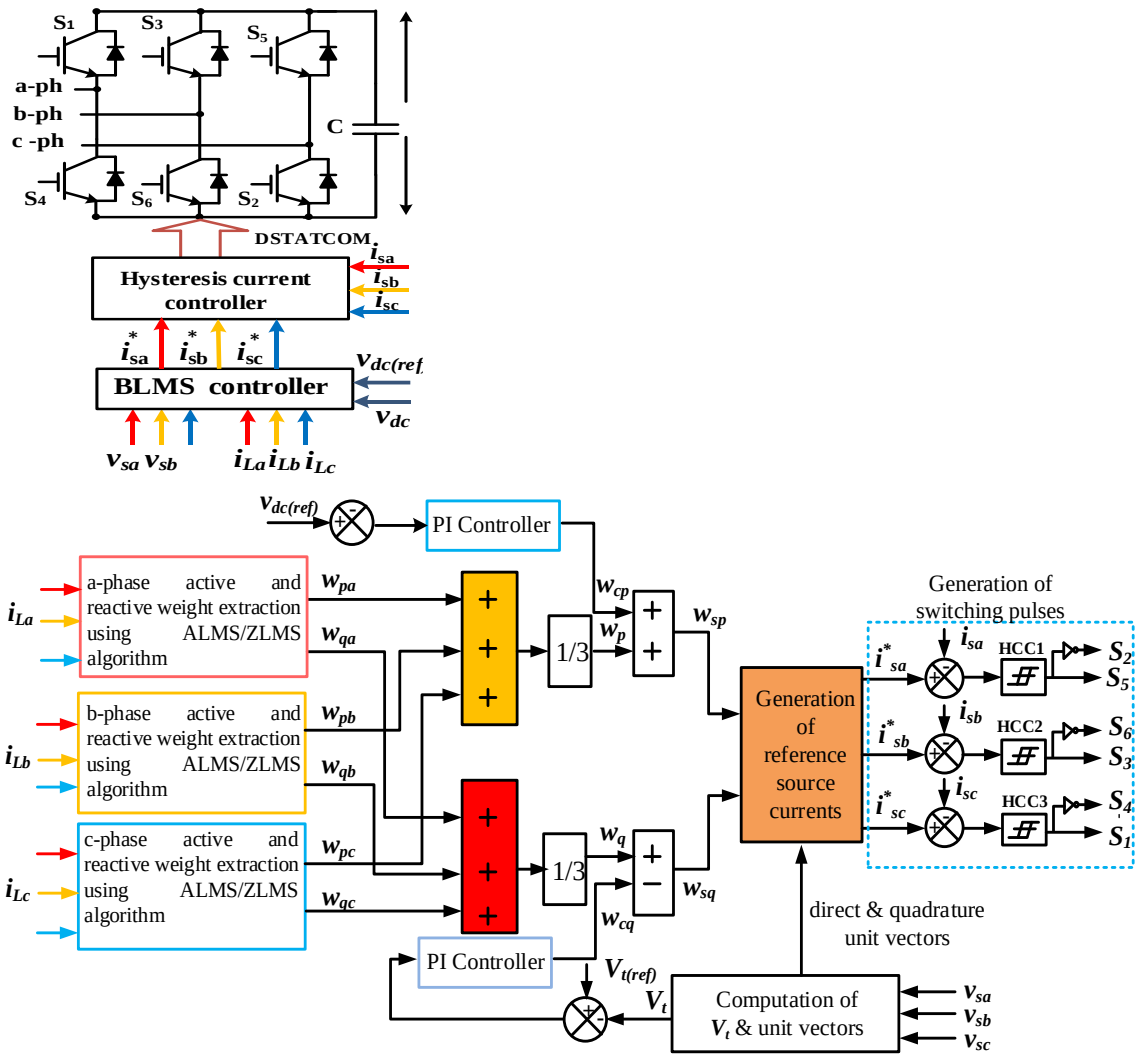

Fig.2. Switching signals generation of VSC utilizing icosϕ control approach

5. Mathematical Formulation of Control Algorithms

Below is a different representation of a quick description of "this control algorithm with regard to its mathematical analysis:

The weighting values extraction of the fundamental active component of a load current (w_{pa}, w_{pb}, w_{pc}) are calculated on the basis of the BLMS controller as mentioned below:

$$w_{pa}(n) = \int w_{pa}(n-1) + \alpha\gamma u_{pa}(n) i_{la}(n) \frac{de_{pa}(n)}{dt} \frac{dE_{pa}(n)}{dt} \quad (1)$$

Whereas $e_{pa}(n) = \alpha\{i_{lpa}(n) - i_{lpA}(n)\}$ and $E_{pa}(n) = \gamma\{i_{la}(n) - w_{pa}(n-1)u_{pa}(n)\}$

$$w_{pb}(n) = \int w_{pb}(n-1) + \alpha\gamma u_{pb}(n) i_{lb}(n) \frac{de_{pb}(n)}{dt} \frac{dE_{pb}(n)}{dt} \quad (2)$$

$$w_{pc}(n) = \int w_{pc}(n-1) + \alpha\gamma u_{pc}(n) i_{lc}(n) \frac{de_{pc}(n)}{dt} \frac{dE_{pc}(n)}{dt} \quad (3)$$

In a similar way, the weighting values of the load current's fundamental reactive component (w_{qa}, w_{qb}, w_{qc}) can be extracted and calculated as

$$w_{qa}(n) = \int w_{qa}(n-1) + \alpha\gamma u_{qa}(n) i_{la}(n) \frac{de_{qa}(n)}{dt} \frac{dE_{qa}(n)}{dt} \quad (4)$$

Whereas $e_{qa}(n) = \alpha\{i_{lqa}(n) - i_{lqA}(n)\}$ and $E_{qa}(n) = \gamma\{i_{la}(n) - w_{qa}(n-1)u_{qa}(n)\}$

$$w_{qb}(n) = \int w_{qb}(n-1) + \alpha\gamma u_{qb}(n) i_{lb}(n) \frac{de_{qb}(n)}{dt} \frac{dE_{qb}(n)}{dt} \quad (5)$$

$$w_{qc}(n) = \int w_{qc}(n-1) + \alpha\gamma u_{qc}(n) i_{lc}(n) \frac{de_{qc}(n)}{dt} \frac{dE_{qc}(n)}{dt} \quad (6)$$

The" computation of the weighting values' mean values (w_a) for the "a, b and c-phase are as mentioned below:

$$w_a = \frac{w_{pa} + w_{pb} + w_{pc}}{3} \quad (7)$$

Similarly, weighting values' mean values (w_r) for the a, b, and c-phases are determined in this way

$$w_r = \frac{w_{qa} + w_{qb} + w_{qc}}{3} \quad (8)$$

C. Computation of in-phase and quadrature unit voltage template

The in-phase unit voltage templates (u_{pa}, u_{pb}, u_{pc}) are the relation of phase voltages as well as PCC voltage amplitude (v_t) determined as mentioned below

$$\boldsymbol{u_{pa} = \frac{v_{sa}}{v_t}, u_{pb} = \frac{v_{sb}}{v_t}, u_{pc} = \frac{v_{sc}}{v_t}} \quad (\mathbf{9})$$

The phase voltage relation is represented by the quadrature unit voltage templates ($\boldsymbol{u_{qa}, u_{qb}, u_{qc}}$) as follows

$$\boldsymbol{u_{qa} = \frac{u_{pb} + u_{pc}}{\sqrt{3}}, u_{qb} = \frac{3u_{pa} + u_{pb} - u_{pc}}{2\sqrt{3}}, u_{qc} = \frac{-3u_{pa} + u_{pb} - u_{pc}}{2\sqrt{3}}} \quad (\mathbf{10})$$

Where$\boldsymbol{v_t}$ can be denoted as

$$\boldsymbol{v_t = \sqrt{\frac{2(v_{sa}^2 + v_{sb}^2 + v_{sc}^2)}{3}}} \quad (\mathbf{11})$$

D. Estimation of the active component of reference source currents

The error in voltage of DC ($\boldsymbol{v_{de}}$) is the" difference between reference as well as measured DC voltages, and it can be written as

$$\boldsymbol{v_{de} = v_{dc\,(ref)} - v_{dc}} \quad (\mathbf{12})$$

The PI (Proportional-Integral) controller procedure these variations in order to regulate the "constant DC bus voltage. The PI controller's output could be written as

$$\boldsymbol{w_{cp} = k_{pa} v_{de} + k_{ia} \int v_{de} dt} \quad (\mathbf{13})$$

The active components' average magnitude of the load currents plus the overall output of the PI controller could be used to express the reference source current overall active components.

$$\boldsymbol{w_{sp} = w_a + w_{cp}} \quad (\mathbf{14})$$

E. Estimation of the reactive component of reference source currents

The error in AC voltage ($\boldsymbol{v_{te}}$) is the difference between the reference AC voltage as well as the observed amplitude of the AC voltage. It could be written as

$$v_{te} = v_{t\,(ref)} - v_t \quad (15)$$

The PI controller processes this difference in order to keep the AC bus voltage constant. The PI controller's output" could be written as

$$w_{cq} = k_{pr} v_{te} + k_{ir} \int v_{te} dt \quad (16)$$

The overall reactive "components of the reference source current could be described as the difference between the PI controller's output and the reactive component average magnitude of the load currents.

$$w_{sq} = w_r - w_{cq} \quad (17)$$

F. Estimation of switching signal generation

The 3-phase instantaneous reference source active component is found by multiplying the active power current component by the in-phase unit voltage template. These results are produced as

$$i_{aa} = w_{sp} u_{pa}, i_{ab} = w_{sp} u_{pb}, i_{ac} = w_{sp} u_{pc} \quad (18)$$

Similar to this, the quadrature unit voltage template, as well as the reactive current component, are multiplied to estimate the 3-phase instantaneous reference source reactive component, and the results are as

$$i_{ra} = w_{sq} u_{qa}, i_{rb} = w_{sq} u_{qb}, i_{rc} = w_{sq} u_{qc} \quad (19)$$

Reference source currents are the total of the current's active along with reactive components; they could be found as

$$i^*_{sa} = i_{aa} + i_{ra}, i^*_{sb} = i_{ab} + i_{rb}, i^*_{sc} = i_{ac} + i_{rc} \quad (20)$$

The both actual source currents (i_{sa}, i_{sb}, i_{sc}) as well as the reference source currents ($i^*_{sa}, i^*_{sb}, i^*_{sc}$) of the respective phases have been compared then current error signals have been fed to an HCC (Hysteresis current controller). Their outputs are utilized to feed the IGBTs (Insulated-Gate Bipolar Transistors) T_1 to T_6 of the VSC served as a" DSTATCOM.

7. Simulation results

A. System performance by utilizing BLMS approach-based DSTATCOM

The distribution system performance BLMS approach on the basis of DSTATCOM under the balanced load has been carried out. The capacitor voltage ($\boldsymbol{v_{dc}}$), compensating current ($\boldsymbol{i_{ca}, i_{cb}, i_{cc}}$), load current ($\boldsymbol{i_{la}, i_{lb}, i_{lc}}$), source current ($\boldsymbol{i_s}$) and source voltage ($\boldsymbol{v_s}$) of the specific distribution system subjected to balance nonlinear load are depicted in Fig. 3. The attained THD of source current as well as load current values by utilizing this control approach are depicted in Fig.4 & 5. The power factor has been enhanced, that can be seen in Fig. 6. But the harmonic compensation of the source current is not suitable as per IEEE 519-1992 as well as IEC 61000-3 standards. The voltage across the self-supported capacitor is 661 Volt has been recorded.

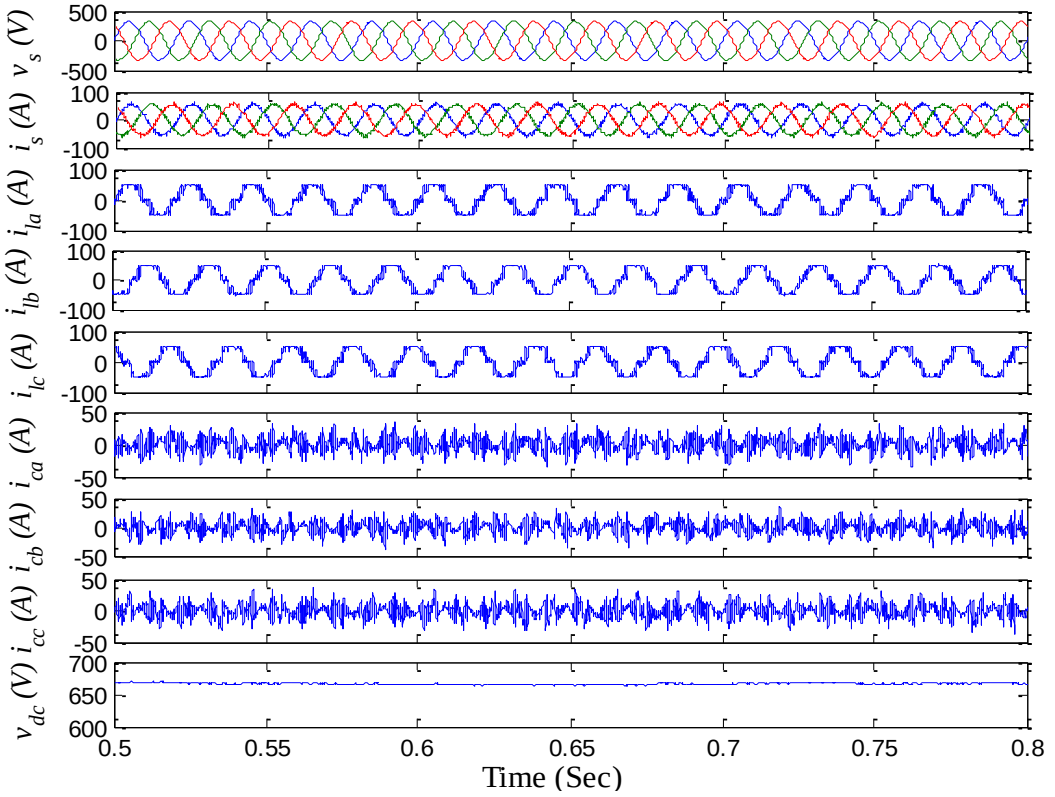

Fig.3. System performance using BLMS technique-based DSTATCOM

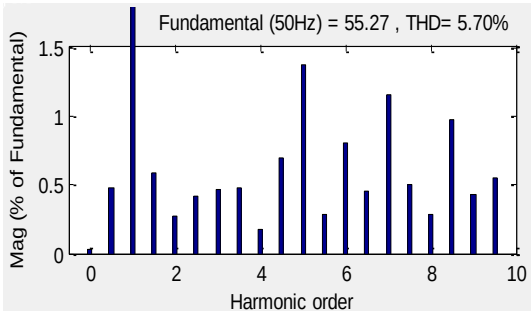

Fig.4 Harmonic spectra of source current

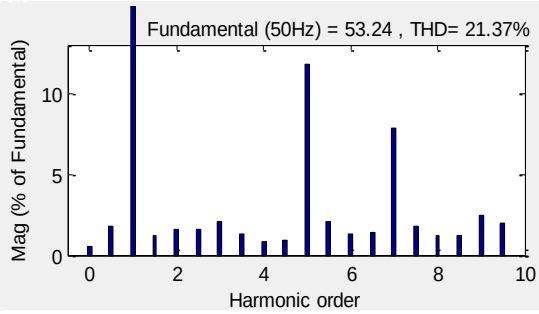

Fig.5 Harmonic spectra of load current

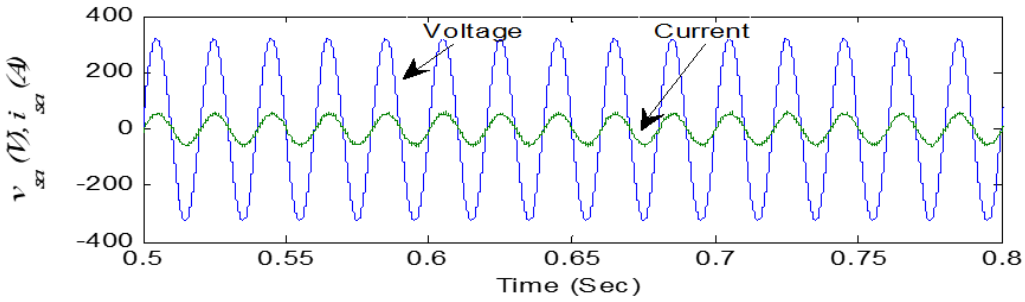

Fig. "6 Waveform of a-phase source voltage and source current

B. System performance utilizing BLMS control technique based DSTATCOM under unbalanced condition

DSTATCOM is run using the distribution system performance BLMS approach while the load is imbalanced. The capacitor voltage (v_{dc}), compensating current (i_{ca}, i_{cb}, i_{cc}), load current (i_{la}, i_{lb}, i_{lc}), source current (i_s) and source voltage (v_s) of the particular distribution system subjected to balance nonlinear load have been displayed in Fig. 7. Figures 8 and 9 display the THD of the source current as well as load current" values that were achieved utilizing this control approach. Figure 10 illustrates the improved power factor. However, the source current's harmonic correction does not meet IEEE 519-1992 and IEC 61000-3 requirements. It is observed that there are 661 volts across the self-supported capacitor.

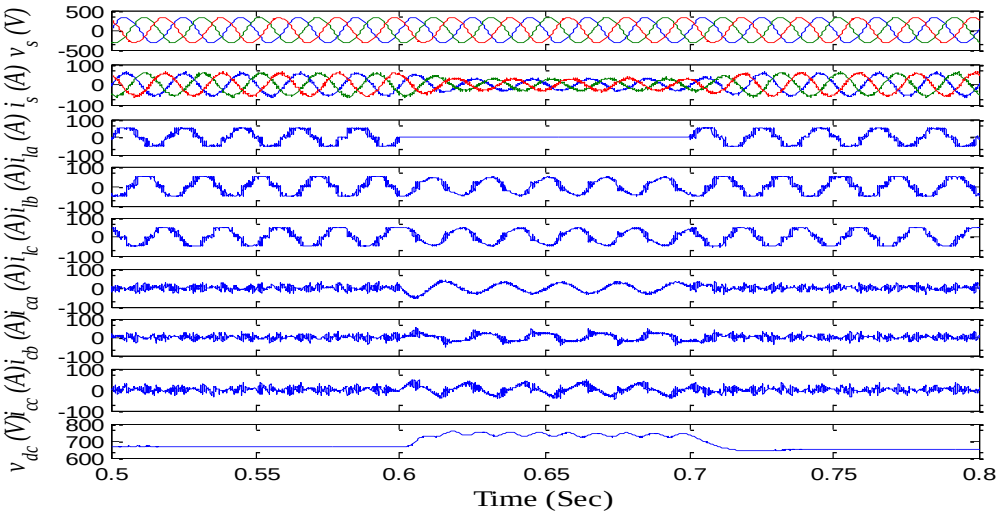

Fig.7. System performance in unbalanced conditions using DSTATCOM based on the BLMS approach

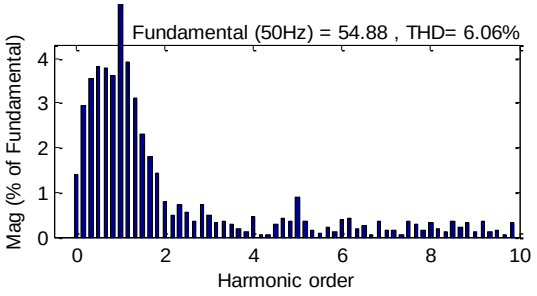

Fig.8 Harmonic spectra of source current

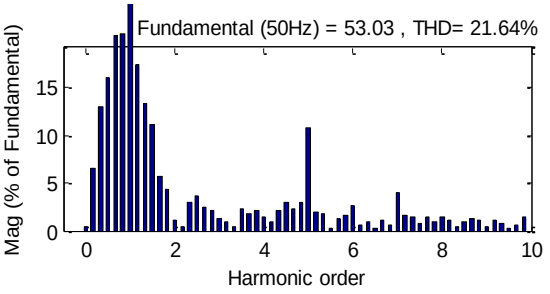

Fig.9 Harmonic spectra of load current

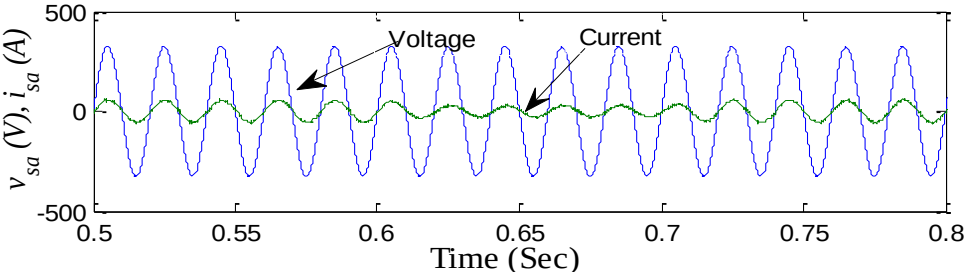

Fig.10 Waveform of a-phase source voltage and source current

Table:1

Grid forming converter	
Rated voltage	230V 50Hz
Sampling and switching frequency	10kHz
Rated power	5kVA
LCL filter	L1=37µH, L2 =500µH, and C1=10µF

Digital signal processor	
Coupling transformer	5 kVA, 24-230V
Dc link voltage	48V

Table:2

Grid forming converter	
Coupling transformer	Star Delta Star
Sampling and switching frequency	10kHz
Active filter	10 kVA
LC filter	Lf=500µH, and Cf=0.5µF
Digital signal processor	SPATRON-6
Dc link capacitor	2000 µF
Capacitor bank	5 kVA, 24-230V
Dc link voltage	48V

8. CONCLUSION

These days, distributed generation (DG) is a major concern. Most distributed generation (DG) implementations are integrated into MGs which could function independently of the main grid and utilize power electronics converters as the front end. These microgrids are more vulnerable to issues with PQ since they have a substantially lower equivalent impedance than the connected power system. When providing nonlinear loads, converter output LCL filters may give rise to harmonic parallel resonance, which lowers microgrid voltage. The operating principle of smart impedance was explained, and experimental research shows that it is a workable way to reduce the unwanted effects of harmonic currents in isolated microgrids. By removing these harmonic currents, the voltage quality of the microgrid is improved by suppressing parallel resonances and reducing voltage distortions. Ultimately, these characteristics can be understood as the conversion, upon reduction of its equivalent impedance, of a weak MG into a quasi-infinite bus. In typical power grids, adding multiple generators in parallel has this effect. To achieve a comparable result, the suggested method can be used without the need for extra generation capacity (active power supply). By only addressing harmonic power, the Smart Impedance achieves a comparable outcome. In contrast to other methods that alter output converter admittance, this one is designed to be a "plug and play" solution that doesn't involve changing converters that are already installed. Furthermore, it offers harmonic droop methods for voltage and current harmonic reduction, something that is rarely accomplished. Because of its shunt connection, the solution does not jeopardize the fundamental functioning of the microgrid in the event of a failure. It has demonstrated resilient operational behavior and a low power rate in relation to load apparent power.

References

1. H. Akagi, Yoshihira Kanazawa, A. Nabae, “Instantaneous reactive power compensators comprising switching devices without energy storage components,” IEEE Trans. Ind. Applicat., 1984, 20 (3), pp. 625-630.
2. H. Haibing and X. Yan, “Design considerations and fully digital implementation of 400-Hz

active power filter for aircraft applications," IEEE Trans. Ind. Electron., 2014, 61 (8), pp. 3823–3834.

3. Y. Hu, Z. Zhu and K. Liu, "Current control for dual three-phase permanent magnet synchronous motors accounting for current unbalance and harmonics," IEEE Trans. Emerg. Sel. Topics Power Electron., 2014, 2 (2), pp. 272-284.
4. M. Aredes, H. Akagi, E.H. Watanabe, E. Vergara Salgado, L.F. Encarnacao, "Comparisons between the p-q and p-q-r theories in three-phase four-wire systems," IEEE Trans. Power Electron., 2009, 24 (4), pp.924-933.
5. B. Wen, D. Boroyevich, R. Burgos, P. Mattavelli and Z. Shen, "Analysis of D-Q small-signal impedance of grid-tied inverters," IEEE Trans. Power Electron., in press, doi: 10.1109/TPEL.2015.2398192.
6. L. Shaohua, W. Xiuli, Y. Zhiqing, L. Tai, P. Zhong, "Circulating current suppressing strategy for MMC-HVDC based on nonideal proportional resonant controllers under unbalanced grid conditions," IEEE Trans. Power Electron., 2015, 30 (1), pp.387-397.
7. X. Guo, W. Liu, X. Zhang, X. Sun, Z. Lu, & J. M. Guerrero, "Flexible control strategy for grid-connected inverter under unbalanced grid faults without PLL," IEEE Trans. Power Electron., 2015, 30 (4), pp. 1773-1778.
8. K. Ma, W. Chen, M. Liserre, F. Blaabjerg, "Power controllability of a three-phase converter with an unbalanced AC source," IEEE Trans. Power Electron., 2015, 30 (3), pp.1591 –1604.
9. M. Castilla, J. Miret, A. Camacho, L. Garcia de Vicuna, J. Matas, "Modeling and design of voltage support control schemes for three-phase inverters operating under unbalanced grid conditions," IEEE Trans. Power Electron., 2014, 29, (11), pp.6139 –6150.
10. S. Srianthumrong, H. Akagi, "A medium-voltage transformerless AC/DC Power conversion system consisting of a diode rectifier and a shunt hybrid filter," IEEE Trans. Ind. Applicat., 2003, 39, pp.874 – 882.
11. W. C. Lee, T. K. Lee, and D. S. Hyun, "A three-phase parallel active power filter operating with PCC voltage compensation with consideration for an unbalanced load," IEEE Trans. Power Electron., 2002, 17(5), pp. 807–814.
12. S. Senini and P.J. Wolfs, "Hybrid active filter for harmonically unbalanced three phase three wire railway traction loads," IEEE Trans. Power Electron., 2000, 15(4), pp.702-710.
13. S. Rahmani, K. Al-Haddad and F. Fnaiech, "A three phase shunt hybrid power filter adopted a general algorithm to compensate harmonics, reactive power and unbalanced load under non ideal mains voltages", Proc. IEEE Int. Conf. on Industrial Technology, IEEE ICIT04, 2004, pp. 651-656.
14. S. Rahmani, A. Hamadi, K. Al-Haddad, "A Lyapunov-Function-Based Control for a Three-Phase Shunt Hybrid Active Filter," IEEE Trans. Ind. Electron., 2012, 59 (3), pp.1418-1429.
15. P. Salmeron and S. P. Litran, "A control strategy for hybrid power filter to compensate four-wires three-phase systems," IEEE Trans. Power Electron., 2010, 25 (7), pp. 1923–1931.
16. J. He, Y. W. Li, R. Wang, and C. Zhang, "Analysis and mitigation of resonance propagation in grid-connected and islanding microgrids," IEEE Trans. Energy Convers., vol. 30, no. 1, pp. 70–81, Mar. 2015.
17. RT-Lab Professional. <http://www.opal-rt.com/product/rt-lab-professional>.
18. A.K Panda and M. Mangaraj, "DSTATCOM employing hybrid neural network control technique for power quality improvement," IET Power Electronics, 2017, 10 (4), pp. 480-489.
19. M. Mangaraj and A. K. Panda, "Performance analysis of DSTATCOM employing various control algorithms," IET Gene., Trans. & Distri., 2017, 11(10), pp. 2643-2653.